

具有肿瘤荧光成像性能的核壳纳米过氧化氢酶模拟物

杨 霞 陈秋云* 宋京宝

(江苏大学化学化工学院, 镇江 212013)

摘要: 运用微波法在硅核壳荧光材料的表面修饰了 2-(二吡啶甲基)丙酸的锰配合物, 获得具有荧光性能的锰-硅核壳纳米结构复合物, 运用 IR, UV, TEM 等方法表征了纳米复合物的结构。H₂O₂ 歧化实验显示锰-硅核壳纳米复合物具有较好的过氧化氢酶模拟特性, 是一种新的纳米过氧化氢酶模拟物。体外细胞荧光成像研究表明 2-(二吡啶甲基)丙酸修饰的纳米球不能进入肿瘤细胞内, 而锰-硅核壳纳米复合物能进入肿瘤细胞内, 具备良好的肿瘤靶向性, 显著提高肿瘤荧光成像效果, 可作为新型的肿瘤成像剂。

关键词: 核壳纳米球; 纳米复合物; 成像; 肿瘤

中图分类号: O627.41

文献标识码: A

文章编号: 1001-4861(2012)01-0164-07

Tumor-Imaging Core-Shell Nano-Models for Catalase

YANG Xia CHEN Qiu-Yun* SONG Jing-Bao

(School of Chemistry and Chemical Engineering, Jiangsu University, Zhenjiang, Jiangsu 212013, China)

Abstract: Microwave synthesis approach has been developed for preparing Mn-silica core-shell nano-complexes with fluorescent imaging by assembling the Mn(II) complexes of bis(2-pyridylmethyl)amino-2-propionic acid (Adpa) on the surface of silica core-shell nanoparticles. IR, UV, TEM were used to characterize the structure of nano-complexes. The results of H₂O₂ disproportionation show that Mn-silica core-shell nano-complexes have good analog characteristics of catalase as a new kind of nano-models for catalase. Cell fluorescence image *in vitro* indicates that these Adpa modified nanoparticles locate outside of tumor cells, in contrast, Mn-silica core-shell nano-complexes could enter tumor cells which enables simultaneous tumor-targeting and good fluorescent imaging as a new tumor imaging agent.

Key words: core-shell nanosphere; nano-complex; imaging, cancer

0 Introduction

Multifunctional nanoparticles with a core-shell architecture, which combine many functionalities such as imaging, targeting, drug delivery, and therapy in a single stable construct, show great promise in biomedical applications^[1-3]. Silica is a hydrophilic material that is photophysically inert and the surface

of the organic-modified silica nanoparticles can be functionalized with a variety of active groups such as amine and carboxyl groups for specific function^[4-5]. Rhodamine B isothiocyanate doped silica-coated core-shell fluorescent dye nanoparticles can specifically recognize early-stage apoptotic cells through the binding of surface conjugated Annexin V to the phosphatidylserine on the outer membrane of apoptotic

收稿日期: 2011-07-06。收修改稿日期: 2011-08-24。

国家自然科学基金 (No.20971059) 资助项目。

*通讯联系人。E-mail: chenqy@ujs.edu.cn

cells^[6]. Manganese(II) ions are the required co-factor for many ubiquitous enzymes and mitochondria can accumulate Mn(II) ions through an ATP-dependent Ca transporter^[7]. The complex of Mn(II)-dpa (dpa=di (picolyl)amines) modified SiO₂@Mn(II)-dpa nanoparticles was used to target cancer cells through intracellular Ca²⁺ signaling mitochondria accumulating *in vivo* for magnetic resonance imaging (MRI) detection^[8]. In addition to attenuation of the absorption of calcium in mitochondria, most transition metal complexes of di(picolyl)amine were reported as models of non-heme dioxygenase^[9]. Manganese(II) complexes [Mn₂(μ-O₂CCH₃)₃L₂]⁺ (L=bis(pyridylmethyl)amine) and aminopyridine manganese(II) complexes were studied for their ability to disproportionate H₂O₂ and to produce highly value intermediates^[10]. These mean that manganese (II) complexes with the derivatives of bis(2-pyridylmethyl)amine could disproportionate H₂O₂ or react with H₂O₂ to produce oxidant. Cellular levels of H₂O₂ play directly or indirectly a key role in malignant transformation and sensitize cancer cells to death. Overpression of H₂O₂-detoxifying enzymes or human catalase *in vivo* can result in H₂O₂ concentration decreasing and cancer cells reverting to normal appearance^[11]. Recently, we found that carboxylate-bridged dimanganese(II) systems were good models for catalase and exhibited good inhibition on the proliferation of U251 and HeLa cells. The inhibiting activity of these manganese (II) complexes on the tumor cells *in vitro* is related to their disproportionating H₂O₂ activity^[12]. It is reported that nano-particles with size of 1~100 nm can accumulate in cancer cells selectively^[13-14]. Here, we report a class of core-shell architecture to assemble the Mn(II) complexes of Adpa (Adpa=bis(2-pyridylmethyl)amino-2-propionic acid) on the surface of silica shell nanoparticles and nano complexes with imaging and mimics of catalase.

1 Experimental

1.1 Instruments and Materials

Rhodamine B isothiocyanate (RBITC), Triton X-100, 3-aminopropyltrimethoxysilane (APTS),

ammonium hydroxide, *N,N*-dicyclohexylcarbodiimide (DCC), *N*-hydroxysuccinimide (NHS), cetyltrimethylammonium bromide (CTAB) and solvents were of analytical grade. Water was purified with a Millipore Milli-Q system (25 °C: 18.2 MΩ·cm, 7.20×10⁻² N·m⁻¹). Rhodamine B isothiocyanate doped silica-coated fluorescent nanoparticles (RBITC@SiO₂) and bis(2-pyridylmethyl)amino-2-propionic acid (Adpa) were prepared according to the reported method^[5,7]. TEM was performed at room temperature on a JEOL JEM-200CX transmission electron microscope using an accelerating voltage of 200 kV. FTIR characterizations were performed using a Nicolet Nexus 470 FTIR spectrophotometer in the spectral range of 4 000 ~ 400 cm⁻¹. The electronic absorption spectrum was recorded using a UV-2450 UV-Vis spectrophotometer at room temperature. Photoluminescent emission spectra were measured on Varian Carry Eclipse spectrofluorometer. The content of Mn(II) ions in the nanoparticle was measured by TAS-986 Atomic absorption spectrophotometer.

1.2 Synthesis of RBITC@SiO₂-Adpa and RBITC@SiO₂-AdpaMn

The Adpa molecules were covalently linked with 3-aminopropyltriethoxysilane (APTS) to form an APTS-Adpa conjugate. DCC was used to ensure that the carboxylic group of Adpa selectively reacts with the amino group of APTS. Adpa (0.1 mL, 0.35 mmol), DCC (22.5 mg, 0.11 mmol) and NHS (40.3 mg, 0.35 mmol) were sequentially added into a 5.0 mL *N,N*-dimethyl-formamide (DMF) solution. The mixture was stirred for 12 h at room temperature. After the filtration, 85.3 mg (0.38 mmol) of APS was added into the solution and the solution was stirred for 24 h at room temperature. The obtained solution was directly used without further treatment.

0.044 8 g Rhodamine B isothiocyanate doped silica-coated fluorescent nanoparticles (RBITC-SiO₂) was dispersed in 25 mL of toluene, 0.1 mL of as-prepared Adpa-APTS conjugates and 20 μL APS were added into the above solution. After the solution was transferred into a flask under nitrogen for 10 minutes, the reaction was allowed to proceed for 1.5 h at 70 °C

in microwave reactor. After centrifuged and washed with ethanol, nanoparticles (RBITC@SiO₂-Adpa) were then obtained.

The obtained RBITC@SiO₂-Adpa (0.485 g) was dispersed in ethanol (25 mL), MnAc₂·4H₂O (0.068 g, 0.014 mmol) was added into the solution and the solution was stirred for 2 h at room temperature. Nanoparticles (RBITC@SiO₂-AdpaMn) were obtained after centrifuging and washing with methanol. The amount of Mn(II) ions in RBITC@SiO₂-dpa-Mn was evaluated by atomic absorption spectra after the nanoparticles were cooked with excess amount of nitric acids at 70 °C for 3 h. The content of Mn(II) in the nanoparticles is 1.13%.

1.3 Catalase-like Activity

All of the reactions between the nano-complexes and dihydrogen peroxide were performed in buffered (Tris/Tris-HCl, 0.1 mol·L⁻¹, NaClO₄ 0.1 mol·L⁻¹, pH=7.1) solutions at 0 °C and 37 °C. The reactivity of the complexes with H₂O₂ was first investigated in buffered solutions via UV-Vis spectroscopy titration at 0 °C and 37 °C. After the solution (5 mL) of nano-complexes (0.1 mol·L⁻¹) was stirred at 0 °C and 37 °C for 30 min, 0.5 mL of H₂O₂ aqueous solution (30%) was added, and the spectra were recorded at 10 min intervals at 0 °C or 2 min intervals at 37 °C. The volumetric measurements of the evolved dioxygen produced during the reaction of the complexes with H₂O₂ were performed in triplicate as follows: a 10 mL round-bottom flask containing a nano-complex (3×10⁻⁴ mol·L⁻¹, 3.0 mL) in a buffered system was placed in an ice (273.0±0.1 K) bath. The flask was closed with a rubber septum, and a cannula was used to connect the reaction flask to an inverted graduated pipet, filled with water. While the solution containing the nano-complex was stirred, a solution of 0.5 mL of H₂O₂ aqueous solution was added through the septum using a microsyringe. The volume of oxygen produced was measured in the pipet. The kinetic measurements for nano-complexes were performed in Tris/Tris-HCl solution at 37 °C. Different concentrations of dihydrogen peroxide were prepared by diluting the 30% H₂O₂ aqueous solution with Tris/Tris-HCl

solution. The optimum reaction order of the substrate with respect to the complexes was determined by reacting different concentrations of complexes with a constant concentration of substrate. Similarly, the optimum reaction order of the complexes with respect to the substrate was determined by reacting different concentrations of substrate with a constant concentration of complexes.

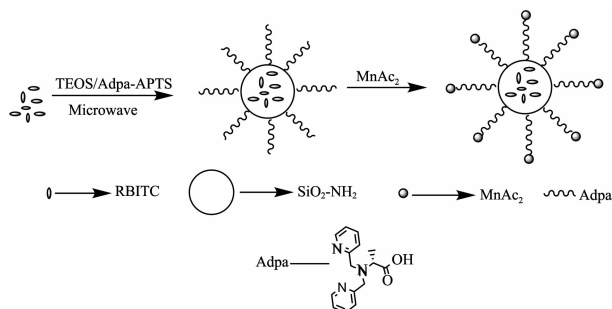
1.4 Cellular uptake and imaging

Human cancer cell line HeLa was obtained from Cancer Cell Repository (Shanghai cell bank). Cells were maintained in RPMI-1640 medium and DMEM medium (Gibco, USA) supplemented with 10% (V/V) heat-inactivated fetal bovine serum, antibiotics (100 U·mL⁻¹ penicillin and 100 U·mL⁻¹ streptomycin), at 37 °C in a humidified atmosphere of 5% CO₂. HeLa cells (2.4×10⁴) were seeded into 24-well plates (Every plate was 100 μL) and cultured for 24 h, then nanoparticles (test nanoparticles (2.0 mg) were dispersed in H₂O and diluted with culture media) were added and incubated for 3 h. At last, cells were washed with PBS twice to remove the free nanoparticles. Nanoparticles uptake and imaging of HeLa cells were observed using Nikon Ti-E2000 microscope with live cell system (LCS) which can provide CO₂, temperature control and position fixing. The bright and fluorescence imaging of cells (ex. 555 nm) were recorded and analyzed.

2 Results and discussion

2.1 Synthesis and characterization

Scheme 1 sketches this synthesis procedure from fluorescent dye molecules towards fluorescence core-shell nano-models for catalase. Normally, reverse



Scheme 1 Synthetic route of RBITC@SiO₂-AdpaMn

microemulsion method was used to prepare rhodamine B isothiocyanate doped silica-coated (RBITC@SiO₂) and further modification of APS derivatives was carried out by refluxing for 24 h in toluene [5]. Although the process is useful, it takes long reaction time and produces by-products that limit bio-applications. Here higher yielded grafted nanomodels were obtained through the microwave synthesis. These indicate that microwave assisted synthesis approach is effective and fast to the modification of silica.

FTIR spectra (Table 1) of the two silica

Table 1 IR bands (cm⁻¹) of RBITC@SiO₂-Adpa and RBITC@SiO₂-AdpaMn

Nanoparticles	$\nu(\text{N-H})$	$\nu(\text{C-H})$	$\nu(\text{CO-NH})$	$\nu(\text{C=C, C=N})$	$\nu(\text{Si-O})$	$\delta(\text{CH, pyridine})$
RBITC@SiO ₂ -Adpa	3 417	2 928	1 659	1 607	1 100	794
RBITC@SiO ₂ -AdpaMn	3 420	2 928	1 659	1 609	1 100	794

The bands at 278 nm of pyridyl rings dominate the UV spectra for RBITC@SiO₂-AdpaMn nanoparticles and RBITC@SiO₂-Adpa nanoparticles confirming the existence of Mn(II)-Adpa grafted silica nanoparticles. 558 nm of π - π^* transition bands belongs to rhodamine B isothiocyanate (Fig.1).

The content of surface modified Adpa in the nano-models is 0.08 mmol · L⁻¹ according to the bands at 278 nm of free Adpa. The emission bands at 582 nm show that the fluorescence intensity of the RBITC@SiO₂-Adpa system little decreases upon the surface modification with Mn (Fig.3 line a). The hypochromism possibly is due to the self-quench of the Mn ions because the transition-metal ions (Mn²⁺)

nanoparticles confirmed the existence of amino in the purified nanoparticles, showing characteristic peaks around 3 417 and 2 928 cm⁻¹ that correspond to stretching bands of N-H and C-H. The IR spectra show pyridyl ring bands of $\nu_{\text{as}}(\text{C=N})$ at approximately 1 609 cm⁻¹ and the $\delta(\text{CH})$ vibration of the pyridyl ring at 794 cm⁻¹. The peaks at 1 659 cm⁻¹ indicates the existence of -CO-NH of Adpa. The strong peaks around 1 100 cm⁻¹ in Table 1 confirm the existence of SiO₂ which corresponds to stretching band of Si-O.

have unsaturated d-layer electrons [14]. However, the fluorescence intensity at 582 nm of RBITC-SiO₂@AdpaMn increases after addition of 0.5 mL - H₂O₂, indicating the nano-complex could possibly bind with H₂O₂ to produce new intermediates. The nanoparticle suspension was added drop-wise onto a carbon-coated copper membrane and dried at room temperature. Particle size was measured with a Hitachi-800 transmission electron microscope. The diameters of RBITC@SiO₂-Adpa and RBITC@SiO₂-AdpaMn are 90~100 nm (Fig.3)

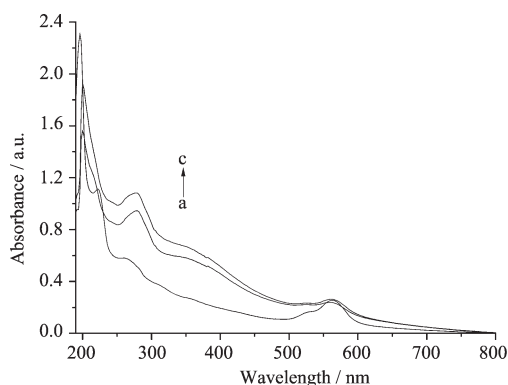


Fig.1 UV spectra for RBITC@SiO₂ (a, 2.1 mg), RBITC@SiO₂-AdpaMn (b, 3.3 mg), RBITC@SiO₂-Adpa (c, 2.9 mg) dispersed in Tris-HCl(pH=7.1)(10 mL)

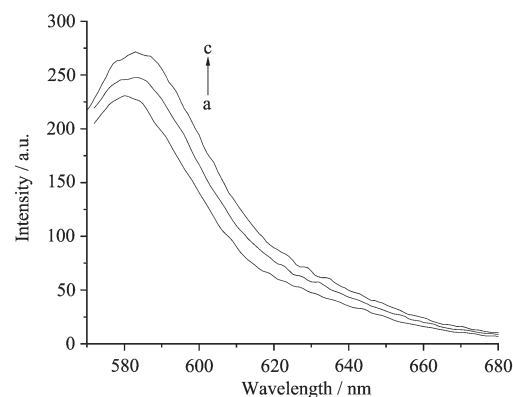
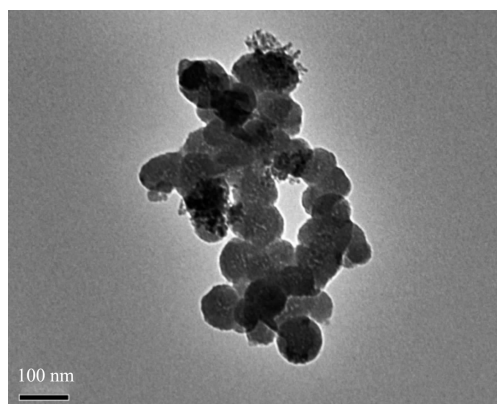
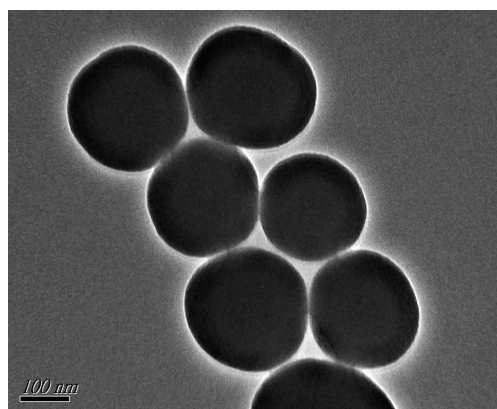


Fig.2 Fluorescence emission spectra for RBITC@SiO₂-AdpaMn (a, 3.3 mg), RBITC@SiO₂-Adpa (b, 2.9 mg) and H₂O₂ added to RBITC@SiO₂-AdpaMn (c, 3.3 mg) in Tris-HCl(pH=7.1) (10 mL), the slit widths at the excitation and emission of the spectrofluorimeter is 5

Fig.3(a) TEM images for RBITC@SiO₂-AdpaMnFig.3(b) TEM images for RBITC@SiO₂-AdpaMn

2.2 Catalase-like activity measured by O₂ evolution -kinetics studies

The O₂ volume evolution was used for the study of kinetic of H₂O₂ disproportionation. The H₂O₂ disproportionation promoted by RBITC@SiO₂-AdpaMn was carried out in Tris-HCl at 0 °C and 37 °C. RBITC@SiO₂-AdpaMn can disproportionate dihydrogen peroxide to generate dioxygen. The volume of oxygen produced every 2 min and the rates of the O₂ evolution of the RBITC@SiO₂-AdpaMn at different conditions are shown in Fig.4.1. The kinetic plot is shown in Fig.4.2 and Fig.4.3. The obtained plot of initial rate vs concentration of the dihydrogen peroxide (E) is fitted by Hill equation [$V_0 = V_{\max} \cdot c_s^n / (K_M + c_s^n)$]. According to the equation, the value of K_M is 0.2150 mmol·L⁻¹, turnover Number K_{cat} calculated from the equation $K_{\text{cat}} = V_{\max} / c_{E, t}$ is 0.5368 s⁻¹ [16]. The value of k_{cat} / K_M is used to evaluate the catalase activity. k_{cat} / K_M of the nano-model is 2 496.7, which shows that the nano-complex has good activity. The

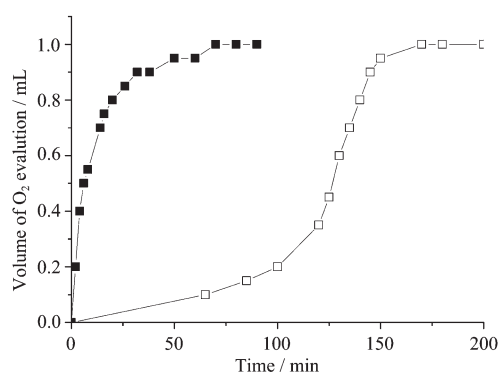


Fig.4.1 Rates of the O₂ evolution for the RBITC@SiO₂-AdpaMn (nano-complex) at different conditions, $c_{\text{nano-complex}} = 0.3 \text{ mmol} \cdot \text{L}^{-1}$, 30% H₂O₂ aqueous solution 0.5 mL, $V_{\text{solvent}} = 3 \text{ mL}$, 37 °C in Tris-HCl (■), 0 °C in Tris-HCl (□)

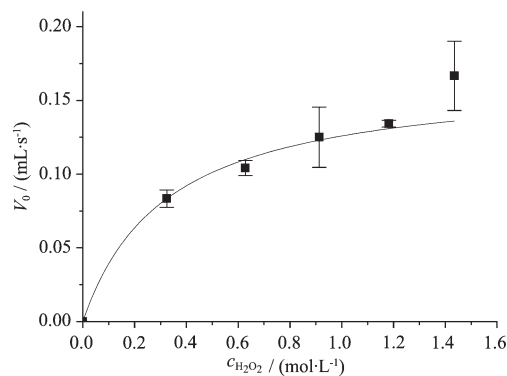


Fig.4.2 V_0 vs Concentration of H₂O₂ plots of RBITC@SiO₂-AdpaMn(0.3 mmol·L⁻¹) in Tris-HCl, 37 °C

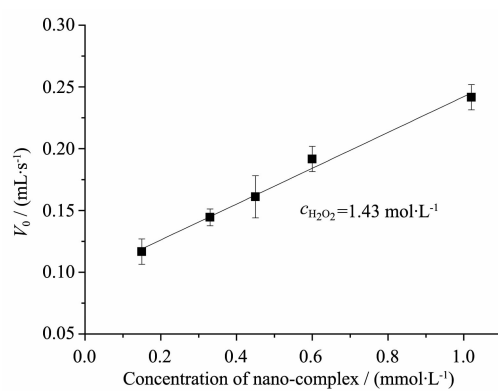


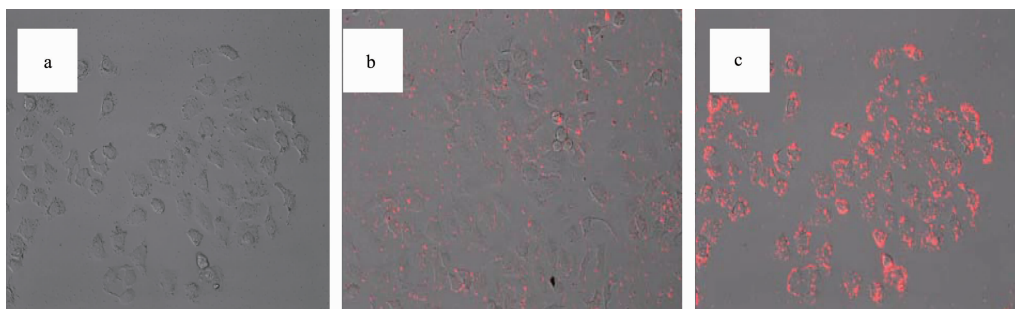
Fig.4.3 Initial rate (V_0) of substrate consumption vs concentration of RBITC@SiO₂-AdpaMn in Tris-HCl 37 °C

condition of the reaction carried out at 37 °C in Tris-HCl solution is mimetic condition of the cell environment. So we deduce that nano-complex would also show good catalase activity *in vitro*.

2.3 Cell uptake and imaging

The fluorescence images of the RBITC@SiO₂-Adpa and RBITC@SiO₂-AdpaMn were assayed using HeLa cell line. For HeLa cells treated with RBITC@SiO₂-Adpa, the red fluorescence image indicates these nanoparticles located outside of HeLa cells due to that the relative larger size and low water solubility result in no internalization of the nontarget control. On the contrary, the intense fluorescence image of cell is observed when HeLa cells incubate with the RBITC@SiO₂-AdpaMn. The results are shown in Fig.5. A total of about 95% of cells display the RBITC signal. All emissions from the nanoparticle containing culture medium surrounding the cells are removed by washing the cells with PBS. Electron

micrographs of the cells provide direct evidence that a large number of RBITC@SiO₂-AdpaMn are possibly endocytosed by the HeLa cells. The mitochondrial membrane potentials of tumor cells are higher than those of normal cells, most agents have a positively charged moiety that takes advantage of electrostatic forces in locating its target^[17]. These preliminary data reveal that the targeting ability of nanospheres to HeLa cells is enhanced greatly due to the Adpa-Mn complex conjugation onto the surface of the RBITC@SiO₂ producing the positive charged RBITC@SiO₂-AdpaMn and allowing passive accumulating and mitochondrial membrane of cancer cells induced accumulation.



A: control; B: RBITC@SiO₂-Adpa; C: RBITC@SiO₂-AdpaMn

Fig.5 Fluorescence images of HeLa cells treated with nanoparticles

3 Conclusions

A Nano-complex (RBITC@SiO₂-AdpaMn) with catalase activity was synthesized and characterized. It is found that the nano-complex could disproportionate H₂O₂ effectively to oxygen, so it is a good mimic of catalase. Furthermore, we found that RBITC@SiO₂-AdpaMn could target and imaging tumor cell by allowing passive accumulating and mitochondrial membrane of cancer cells induced accumulation.

References:

- [1] Sanvicens N, Marco M P. *Trends Biotechnol.*, **2008**,**26**(8):42-433
- [2] Wu W T, Shen J, Banerjee P, et al. *Biomater.*, **2010**,**31**(29): 7555-7566
- [3] Zhang R R, Wu C L, Tong L L, et al. *Langmuir*, **2009**,**25** (17):10153-10158
- [4] Bonacchi S, Genovese D, Juris R, et al. *Angew. Chem. Int. Ed.*, **2011**,**50**(18):4056-4066
- [5] Tao G P, Chen Q Y, Yang X, et al. *Colloids Surf. B: Biointerf.*, **2011**,**86**(1):106-110
- [6] Shi H, He X X, Wang K M, et al. *Nanomed. Nanotechnol. Biol. Med.*, **2007**,**3**(4):266-272
- [7] Chen Q Y, Zhou D F, Huang J, et al. *J. Inorg. Biochem.*, **2010**,**104**(11):1141-1147
- [8] Chen Q Y, Wang L Y, Zhang L R, et al. *Sci. China Chem.*, **2010**,**53**(8):1728-1731
- [9] CHEN Qiu-Yun(陈秋云), HUANG Juan(黄娟), LI Jun-Feng (李军峰), et al. *Chinese J. Inorg. Chem. (Wuji Huaxue Xuebao)*, **2008**,**24**(11):1789-1793
- [10] Romero I, Dubois L, Collomb M N, et al. *Inorg. Chem.*, **2002**,**41**(7):1795-1806
- [11] López-Lázaro M. *Cancer Lett.*, **2007**,**252**(1):1-8
- [12] Zhou D F, Chen Q Y, Qi Y, et al. *Inorg. Chem.*, **2011**, doi.

- org/10.1021/ic200004y
- [13]Bahadur N M, Furusawa T, Sato M, et al. *J. Colloid Interf. Sci.*, **2011**,**355**(2):312-320
- [14]CHEN Qiu-Yun(陈秋云), WANG Lin-Yun(王玲昀), CHEN Hao(陈浩), et al. *Chinese J. Inorg. Chem. (Wuji Huaxue Xuebao)*, **2010**,**26**(10):1784-1789
- [15]Groni S, Blain G, Guillot R, et al. *Inorg. Chem.*, **2007**,**46**(6): 1951-1953
- [16]Shin B K, Kim M Y, Han J H. *Polyhedron*, **2010**,**29**(12): 2560-2568
- [17]Jasuja K, Linn J, Melton S, et al. *J. Phys. Chem. Lett.*, **2010**,**1**(12):1853-1860